ANNALS of Clinical and Translational Neurology
Open Access
ANA American Neurological Association since 1875

RESEARCH ARTICLE

Electrophysiological biomarkers in spinal muscular atrophy: proof of concept

W. David Arnold[1,2], Paul N. Porensky[3], Vicki L. McGovern[4], Chitra C. Iyer[4], Sandra Duque[4], Xiaobai Li[5], Kathrin Meyer[6], Leah Schmelzer[6], Brian K. Kaspar[6,7], Stephen J. Kolb[1,4], John T. Kissel[1,7] & Arthur H. M. Burghes[1,4]

[1]Department of Neurology, The Ohio State University Wexner Medical Center, 395 W. 12th Ave, Columbus, Ohio 43210
[2]Department of Physical Medicine and Rehabilitation, The Ohio State University Wexner Medical Center, 480 Medical Center Drive, Columbus, Ohio 43210
[3]Department of Neurosurgery, The Ohio State University Wexner Medical Center, 410 West 10th Avenue, Columbus, Ohio 43210
[4]Department of Molecular and Cellular Biochemistry, The Ohio State University Wexner Medical Center, 363 Hamilton Hall, 1645 Neil Ave, Columbus, Ohio 43210
[5]Center for Biostatistics, The Ohio State University, Columbus, Ohio 43210
[6]Nationwide Children's Hospital Research Institute, Columbus, Ohio 43205
[7]Department of Pediatrics, The Ohio State University, Columbus, Ohio 43210

Correspondence
W. David Arnold, 395 W. 12th Ave, Columbus, OH 43210. Tel: 614-293-4969; Fax: 614-293-6111; E-mail: william.arnold@osumc.edu

Funding Information
This study was supported by funding from NIH 5K12HD001097-17 to W. D. A., the Swiss National Science Foundation to K. M., NIH/NINDS U01NS080836 to B. K. K., Families of SMA to B. K. K., Sophia's cure to B. K. K., NIH/NINDS K08NS067282 and U01NS079163 to S. J. K., and NIH HD006508 to A. H. M. B.

Received: 13 September 2013; Revised: 9 November 2013; Accepted: 12 November 2013

***Annals of Clinical and Translational Neurology* 2014; 1(1): 34–44**

doi: 10.1002/acn3.23

Abstract

Objective: Preclinical therapies that restore survival motor neuron (SMN) protein levels can dramatically extend survival in spinal muscular atrophy (SMA) mouse models. Biomarkers are needed to effectively translate these promising therapies to clinical trials. Our objective was to investigate electrophysiological biomarkers of compound muscle action potential (CMAP), motor unit number estimation (MUNE) and electromyography (EMG) using an SMA mouse model. **Methods**: Sciatic CMAP, MUNE, and EMG were obtained in SMNΔ7 mice at ages 3–13 days and at 21 days in mice with SMN selectively reduced in motor neurons ($ChAT^{Cre}$). To investigate these measures as biomarkers of treatment response, measurements were obtained in SMNΔ7 mice treated with antisense oligonucleotide (ASO) or gene therapy. **Results**: CMAP was significantly reduced in SMNΔ7 mice at days 6–13 ($P < 0.01$), and MUNE was reduced at days 7–13 ($P < 0.01$). Fibrillations were present on EMG in SMNΔ7 mice but not controls ($P = 0.02$). Similar findings were seen at 21 days in $ChAT^{Cre}$ mice. MUNE in ASO-treated SMNΔ7 mice were similar to controls at day 12 and 30. CMAP reduction persisted in ASO-treated SMNΔ7 mice at day 12 but was corrected at day 30. Similarly, CMAP and MUNE responses were corrected with gene therapy to restore SMN. **Interpretation**: These studies confirm features of preserved neuromuscular function in the early postnatal period and subsequent motor unit loss in SMNΔ7 mice. SMN restoring therapies result in preserved MUNE and gradual repair of CMAP responses. This provides preclinical evidence for the utilization of CMAP and MUNE as biomarkers in future SMA clinical trials.

Introduction

Spinal muscular atrophy (SMA), an autosomal recessive motor neuron disorder, is the most common hereditary cause of death in infants.[1] SMA is caused by functional loss of the *survival motor neuron 1* (*SMN1*) gene,[2] and the retention of a second similar gene, *SMN2*. *SMN2* differs from *SMN1* by a single nucleotide in exon 7 that does not change an amino acid but does alter a modulator of splicing.[3–5] This alteration of splicing causes exon 7 to be absent in ~90% of *SMN2* transcripts. This shortened isoform of SMN protein does not oligomerize efficiently and is rapidly degraded[6,7] resulting in reduced SMN protein levels insufficient for normal motor neuron function and survival. *SMN2* copy number and the amount of full length SMN protein influence disease phenotype, with

higher *SMN2* copy number and greater ability to produce full-length SMN associated with milder forms of SMA.[8,9] The downstream targets of SMN deficiency that lead to motor neuron dysfunction and loss are unknown and controversy persists on the exact SMN function affected to cause SMA.[10] SMN not only acts to assemble Sm proteins onto snRNAs[11], but may also be critical in the transport of select mRNAs in axons.[12–14] Currently, there are no clear downstream targets of SMN deficiency that have shown the ability to markedly improve the SMA phenotype in SMA mouse models.

An important model of SMA is the SMNΔ7 mouse, a triple mutant with targeted mutation of the mouse *Smn* gene and two transgenes: two copies of the human *SMN2* gene and a transgene that expresses SMN lacking exon 7 (Δ7).[15] The SMNΔ7 mouse is phenotypically normal at birth, develops progressive weakness starting at postnatal day (PND) 5–6 and dies at approximately 2 weeks of age.[15,16] Several full length SMN protein restoring approaches such as gene replacement, antisense oligonucleotide (ASO) therapy to correct the aberrant splicing pattern, and small molecule therapies have been shown to effectively reduce motor neuron loss and extend survival when mice are treated at early postnatal time points. However, delayed SMN restoration results in diminished response.[17,18] Translating these promising therapies from bench to bedside is hindered by (1) the lack of understanding of downstream targets of SMN deficiency and (2) the lack of understanding of the exact timing of SMN requirement. SMN restoration in patients with SMA could have a dramatic effect provided that SMN is delivered to the correct tissues at a sufficient dose and at the correct time.[19]

SMA is a phenotypically heterogeneous disorder with variable disease onset and severity, which create a series of issues in the design of clinical trials. Sensitive and accurate biomarkers are therefore needed that can be used as predictive, prognostic, and surrogate endpoint measures. Furthermore, biomarkers that can link preclinical findings to clinical understanding are particularly important. Application of translational biomarkers in preclinical models can help predict what will occur in early clinical trials. Preclinical testing in animal models can provide the framework for the design and testing of candidate biomarkers. Using similar or parallel biomarkers in animal models in vivo and in early clinical trials can provide an important link to increase translatability.

Electrophysiological measurements such as the compound muscle action potential (CMAP) and motor unit number estimation (MUNE) can monitor the functional status of the motor unit pool and are particularly pertinent to motor neuron disorders. CMAP response measures the output of the motor units supplying a particular muscle or group of muscles. CMAP size is determined by the size and number of depolarized muscle fibers following supramaximal nerve stimulation. MUNE is an electrophysiological method that can measure the number of motor units supplying a particular muscle. In patients with SMA, needle electromyography (EMG) demonstrates changes of fibrillation potentials (denoting active denervation) and enlarged motor unit action potentials with neurogenic recruitment.[20,21] Cross-sectional studies have shown that CMAP, MUNE, and EMG correlate with other measures of motor function, clinical severity, and overall function (Table 1).[20–25] Importantly, electrophysiological studies have rarely been obtained in early symptomatic or presymptomatic cases, but in the four patients described, electrophysiological measures appear to be preserved prior to onset of overt motor weakness.[22,25] Prior to molecular diagnosis, EMG was an important aspect of clinical diagnosis and remains an important tool in atypical or non-5q related SMA. CMAP, MUNE, and EMG have not been fully defined in SMA mouse models. The potential of these measures includes the ability to assess the output of the motor unit in vivo (Figure S1) and the ability to provide parallel measures in mouse and human and thus predict outcomes in early clinical trials. Our objective was to develop techniques that would permit the measurement of CMAP and MUNE to assess motor unit function in the SMNΔ7 mouse. These studies were designed for assessment during the early postnatal period in mice as small as 1–2 g in an effort to understand motor unit function prior to onset of overt motor weakness. We then used these markers to understand the biological effects of preclinical therapeutics that restore SMN protein levels and seek insight regarding the potential function of CMAP and MUNE as surrogate endpoints.

Table 1. Electrophysiological findings in patients with SMA after onset of overt clinical signs of weakness.

			Electromyography		
	CMAP	MUNE	Fibrillations	Decreased recruitment	Enlarged motor units
Type 1	↓↓↓	↓↓↓	++	↑↑↑	↑
Type 2	↓↓	↓↓	+	↑↑	↑↑
Type 3	↓ or normal	↓	+/–	↑	↑↑↑

SMA, spinal muscular atrophy; CMAP, compound muscle action potential; MUNE, motor unit number estimation.

Materials and Methods

Animals

SMNΔ7 mice (*SMN2*+/+; *SMNΔ7*+/+; *Smn*−/−) were generated by crossing phenotypically normal heterozygote mice (*SMN2*+/+; *SMNΔ7*+/+; *Smn*+/−).[15] Heterozygote mice (*SMN2*+/+; *SMNΔ7*+/+; *Smn*+/−) were used as control animals. SMNΔ7 mice are indistinguishable from controls at birth but develop progressive signs of weakness with an average lifespan of 13.3 days.[15,16] Electrophysiological assessment shows impairment of synaptic vesicle release during neuromuscular junction (NMJ) recordings ex vivo.[26,27] Histological findings include loss of innervation of neuromuscular synapses, reduced muscle fiber size, and moderate motor neuron loss at 9 days.[15]

Additional mice with $ChAT^{Cre}$ promoter (Jackson Laboratory Stock #006410, Bar Harbor, ME, USA)-driven deletion of the Smn^{F7} allele were used to be compared to control mice at 21 days.[28,29] The cross is performed such that the resultant SMA mice possess one Smn^{F7} allele (Jackson Laboratory Stock #006138) and one allele *Smn*2A (null for SMN production) with B galactosidase inserted into exon 2A.[30] Utilizing the *Cre-lox* system, $ChAT^{Cre}$ mice have selectively reduced levels of SMN protein in motor neurons (levels produced by two copies of *SMN2*) in motor neurons and other cells have control levels of SMN. This leads to a phenotype of motor weakness but prolonged survival compared with SMNΔ7 mice.

Anesthesia and animal preparation

Mice were anesthetized using inhaled isoflurane and placed prone on a polystyrene platform with hind limbs extended at the knees and abducted at the hips with adhesive tape. O_2 flow was set at 1 L/min and the percentage isoflurane adjusted for adequate sedation as determined by lack of mouse response to light cutaneous pressure applied by forceps to a hind limb. Care was taken to avoid oversedation. Surface temperature was maintained between 30 and 34°C. Hair growth appears in the neonatal mice at approximately day 7 and 8. The fur of the right hind limb was carefully removed using fine-bladed clippers as needed to allow adequate surface electrode-skin contact (Oster, McMinnville, TN).

Electrophysiological studies

Electrophysiological measurements were performed in SMNΔ7 and control mice at ages 3–13 days. Similar electrophysiological measurements were obtained in $ChAT^{Cre}$ and control mice at 21 days to assess the effects of selective reduction of SMN protein in motor neurons. This also enabled CMAP and MUNE measurements in SMA mice after polyneuronal innervation elimination has occurred.[31] To assess the effects of early SMN restoration, CMAP and MUNE were assessed at day 12 and 30 in mice treated with ASO therapy on day 0 (to increase SMN protein levels) for comparison with controls and untreated SMNΔ7 mice. Measurements were obtained by a single evaluator (W. D. A.) blinded to genotype and treatment status. Nerve conduction studies were performed using a portable electrodiagnostic system (Synergy EMG machine; Oxford Instruments, Abingdon, UK). Waveforms were displayed on an LCD monitor (Toshiba North America, Houston, TX).

Sciatic CMAP and MUNE

Sciatic CMAP and MUNE responses were recorded from the right hind limb while stimulating the sciatic nerve using techniques that are similar to those applied in mouse models of amyotrophic lateral sclerosis and neuropathy with modifications in recording, stimulating electrodes, and filter settings.[32–35] The recording set up is diagramed in Figure 1A. The low pass filter was set at 20 Hz and the high-pass filter at 10 kHz. A pair of insulated 28 or 30 gauge monopolar needles (Teca, Oxford Instruments Medical, NY) were used as the cathode and anode to stimulate the sciatic nerve in the proximal hind limb. These two stimulating electrodes were taped together at the needle hub with a spacing of 2–3 mm between electrode tips for improved one-handed control and localized stimulation. A pair of fine ring wire electrodes (Alpine Biomed, Skovlunde, Denmark) were used for the active (E1) and reference (E2) recording electrodes. The active recording electrode (E1) was placed distal to the knee joint over the proximal portion of the gastrocnemius and the reference electrode (E2) over the metatarsal region of the foot. The loop end of the active and reference electrodes were placed to maximize contact with the posterior limb (E1) and plantar surface of the foot (E2) and held in place using alligator clips attached to ball and socket armatures held secure with an iron base (Helping Hands by RadioShack, Fort Worth, TX). This positioning was crucial to obtain consistent and maximal results. Using this recording setup, it is likely that responses from many sciatic-innervated muscles contribute to the CMAP response, not only those directly under the E1 electrode.[36] In order to reduce impedance, the area of skin contact with the ring electrodes was precisely coated with electrode gel (Spectra 360 by Parker laboratories, Fairfield, NJ) using an irrigating syringe (Covidien, Mansfield, MA). A disposable strip electrode (Carefusion, Middleton, WI) was placed on the contralateral hind limb

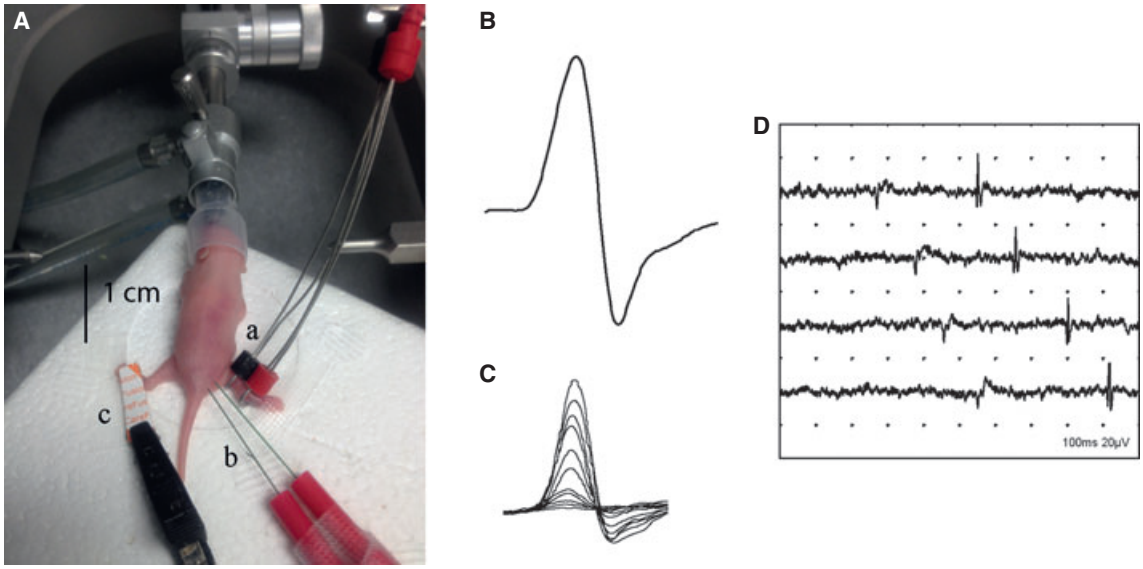

Figure 1. Sciatic CMAP, incremental MUNE, and electromyography. (A) Anesthesia rig with adapted nose cone and electrode placement for sciatic CMAP and MUNE (a, recording electrodes; b, ground electrode; c, stimulating electrodes). (B) Sciatic CMAP response with expected biphasic, initial negative morphology. (C) Ten superimposed incremental MUNE responses with similar biphasic morphology. (D) Fibrillation potentials from an end-stage SMNΔ7 mouse (13 days). CMAP, compound muscle action potential; MUNE, motor unit number estimation; SMN, survival motor neuron.

or tail. The sciatic nerve was stimulated with single square-wave pulses of 0.1-msec duration.

Supramaximal CMAP responses (Fig. 1B) were generated with stimulus currents <10 mA. Baseline-to-peak amplitude measurements were used for comparison of SMNΔ7 and control mice. To assess for failure of NMJ transmission, repetitive CMAP responses were recorded following a train of 10 stimuli at a frequency of 3 Hz. If amplitude was diminished during repetitive stimuli by greater than 10%, then decrement was determined to be present. Sciatic MUNE was performed using an incremental stimulus technique with modifications of electrodes used for stimulation and recording and filter settings.[32] The sciatic nerve was stimulated submaximally to obtain a minimal all-or-none response. The position of the stimulating electrodes was adjusted so that an initial motor response was obtained with <0.7 mA stimulus intensity. If a response was stable, established by observing three duplicate responses, it was stored. Then, the stimulus intensity was gradually increased to record and store a total of 10 incremental responses (Fig. 1C). The peak-to-peak amplitude of each individual motor unit response was calculated by subtracting the amplitude of the prior response. The 10 incremental values were averaged to estimate average single motor unit potential (SMUP) amplitude. The maximum CMAP amplitude (peak-to-peak) was divided by the average SMUP amplitude to yield the estimated number of motor units (MUNE).

Needle EMG

Hind limb muscles were assessed with needle EMG to investigate active denervation of muscle fibers. A 30 gauge concentric needle electrode (Natus, San Carlos, CA) was inserted into distal leg (lateral gastrocnemius) and proximal thigh muscles (biceps femoris). Small amplitude insertions were used to trigger fibrillation potentials. Fibrillation potentials were identified and carefully discerned from endplate spikes by initial positive deflection and regular rate of firing (Fig. 1D). Settings for the high and low frequency filters were set at 20 Hz to 10 kHz, respectively.

Intracerebroventricular ASO therapy and *AAV9* gene therapy to restore SMN levels

SMNΔ7 mice were injected on PND 0 with 40 μg of morpholino ASOs directed against ISS-N1 to increase full length SMN protein production from *SMN2* as previously described by Porensky et al.[37] This preclinical treatment increases median lifespan of the SMNΔ7 mouse from 2 weeks to over 100 days with a single injection.[37] Injected mice underwent electrophysiological measurements at PND 12 and 30 for comparison with untreated SMNΔ7 mice and controls. Similarly, SMNΔ7 mice were treated with a self-complementary adeno-associated virus 9-based vector (2.7×10^{10} viral genomes) containing the

SMN cDNA via intracerebroventricular (ICV) injection at day PND 1, and electrophysiological measurements were obtained at day 165 and compared to control mice.

Statistical analysis

For untreated SMNΔ7 and normal control mice, mean profile plots for CMAP and MUNE were generated. Linear mixed effects models were used to examine the group difference in these measures over time. These models will take the correlation among the measures from the same mouse into account. After examining the model residual plots, square root transformation was chosen for CMAP and log transformation was chosen for MUNE to calculate the *P*-values for the group comparisons. When comparing MUNE and CMAP at day 12 between the treated SMA, the control, and the untreated SMA mice, Wilcoxon ranked sum test was used. Statistical analyses were conducted in SAS (version 9.2, SAS Institute Inc., Cary, NC).

Results

Electrophysiological measurements without rescue

CMAP and MUNE measurements were obtained in untreated SMNΔ7 mice ($n = 8$) and control mice ($n = 8$) at days 3–13 to understand the natural history of motor unit function prior to overt onset of motor weakness and continuing through end-stage disease (Table 2). CMAP amplitudes increased during the early postnatal period in both controls and SMNΔ7 mice similar to humans during early development.[38] Increasing CMAP amplitude may be partly due to increasing muscle fiber size, but prior work has shown static muscle fiber size in SMNΔ7 mice compared with controls.[39] Therefore factors, other than muscle fiber size alone, are contributing to the CMAP response. CMAP amplitudes in SMNΔ7 mice were similar to controls at early time points and significantly reduced starting at day 6 ($P < 0.01$) (Fig. 2A). There was no statistical difference in group-by-time interaction in CMAP responses measured in SMNΔ7 and control mice ($P = 0.33$). Comparison of CMAP amplitudes between SMNΔ7 and control mice between day 7 and 10 showed divergence, but at later time points CMAP amplitude partly recovered consistent with expanded single motor unit territory. CMAP responses following trains of 10 supramaximal repetitive stimulations at 3 Hz demonstrated abnormal NMJ transmission (>10% decrement in amplitude) in 5 of 11 SMNΔ7 mice (ages 7–13 days, mean 8.9 days) and 1 of 10 controls (ages 7–13 days, mean 8 days) ($P = 0.09$).

MUNE in SMNΔ7 mice were similar to control animals at early time points (days 3–5) with reduction starting at 6 days and reaching statistical significance at day 7 ($P < 0.01$) (Fig. 2B). There was a significant difference in group-by-time interaction in MUNE ($P < 0.0001$). Similar to findings in patients with SMA,[20,21] electromyographic assessment of hind limb muscles (biceps femoris and lateral gastrocnemius) at 10–12 days demonstrated fibrillation potentials in 6 of 7 SMNΔ7 mice and 0 of 5 control mice. This is consistent with the presence of active denervation at late stages in the SMNΔ7 mouse (Table 3). Fibrillations in SMNΔ7 mice are very small in amplitude (Fig. 1D), likely due to reduced muscle fiber size. Together, CMAP, MUNE, and EMG findings showed electrophysiological evidence of a presymptomatic period in SMNΔ7 mice with motor unit dysfunction starting at approximately PND 6.

During the early postnatal period there is polyneuronal innervation of muscle fibers in the SMNΔ7 mouse.[40,41] Importantly, in the mouse this exuberant innervation is functional and increases synaptic output of each motor unit 10-fold at birth. Therefore, polyneuronal innervation causes an apparent reduction in MUNE measurements due to overlapping territories of motor units.[31] In contrast, the existing evidence from a single study in humans suggests that monosynaptic innervation is evident at birth.[42] However, further studies are required to be absolutely certain that this is the case. In mice, polyneuronal innervation is eliminated by ~13 days.[31] Figure 3A demonstrates the correlation of the rate of polyneuronal innervation pruning reported by Tapia et al. with the rising MUNE values in control mice in this study.[31] The rate of pruning has been reported to be similar in SMNΔ7 mice and controls in the gastrocnemius[43] and soleus,[39] but others have shown differences in the tibialis anterior[26] and sternomastoid.[39] The minimal rise of MUNE measurements over the first 2 weeks of life in SMNΔ7 mice compared to rising estimates in controls is consistent with falling numbers of functional motor units in the SMNΔ7 mice compared with stable populations in controls (Fig. 3B). This assumes that the rate of pruning is similar in SMNΔ7 and controls in the muscles assessed by our MUNE technique.

Electrophysiological measurements in mice with reduced level of SMN in motor neurons

Electrophysiological measurements were obtained at 21 days in $ChAT^{Cre}$ mice after polyneuronal innervation pruning is complete. Similar to findings in SMNΔ7 mice, these measures demonstrated reduced CMAP amplitude

Table 2. Raw longitudinal CMAP and MUNE measurements in SMNΔ7 and control mice at postnatal days 3–13.

Age (days)	Weight[1] Mean ± SEM	CMAP (mV) Mean ± SEM	CMAP (mV) Minimum	CMAP (mV) Maximum	MUNE Mean ± SEM	MUNE Minimum	MUNE Maximum	MUNE ratio[2]
3	2.3 ± 0.2	2.5 ± 0.3	1.1	4	43 ± 4	24	63	0.89
	2.7 ± 0.1	4.4 ± 0.4	2.4	6.3	48 ± 11	15	120	
4	2.5 ± 0.2	3.9 ± 0.3	2.5	5.9	54 ± 8	32	91	0.97
	3.1 ± 0.1	5.0 ± 0.4	3.4	6.9	56 ± 5	33	79	
5	2.9 ± 0.2	4.6 ± 0.4	3.1	6.6	64 ± 4	50	80	0.93
	3.6 ± 0.1	6.6 ± 0.6	4.2	9.5	69 ± 11	30	114	
6	3.2 ± 0.1	4.8 ± 0.5	3.1	6.7	54 ± 4	44	78	0.70
	4.1 ± 0.1	6.9 ± 0.5	4.4	9.3	78 ± 4	60	103	
7	3.5 ± 0.1	6.7 ± 0.7	4.5	10	59 ± 12	23	134	0.59
	4.7 ± 0.1	9.6 ± 0.3	8.7	11.8	99 ± 9	64	142	
8	3.8 ± 0.1	6.2 ± 0.8	2.9	10.4	57 ± 7	31	105	0.38
	5.2 ± 0.1	12.7 ± 1.8	4.4	19.7	152 ± 23	50	279	
9	4.0 ± 0.1	8.1 ± 0.9	4.8	13.1	56 ± 8	34	98	0.33
	5.8 ± 0.1	16.3 ± 2.2	8.8	27.4	171 ± 23	88	287	
10	3.8 ± 0.2	9.6 ± 0.6	7.1	12	65 ± 8	38	92	0.33
	6.3 ± 0.1	17.1 ± 0.8	12.2	19.7	199 ± 20	143	317	
11	3.6 ± 0.2	14.8 ± 1.3	8.8	19.1	60 ± 7	28	92	0.27
	6.8 ± 0.2	19.7 ± 0.8	15.7	24	225 ± 28	115	320	
12	3.3 ± 0.2	17.0 ± 1.6	7.5	22.5	44 ± 6	19	83	0.18
	7.2 ± 0.2	21.6 ± 0.9	17.5	26.3	241 ± 33	106	349	
13	3.0 ± 0.1	19.2 ± 0.9	16	23.3	61 ± 7	28	87	0.26
	7.4 ± 0.3	24.54 ± 1.2	20.1	31.7	235 ± 25	129	347	

MUNE ratio, SMNΔ7 MUNE/Control MUNE to correct for polyneuronal innervation. SMNΔ7: shaded; Control: unshaded. CMAP, compound muscle action potential; MUNE, motor unit number estimation; SMN, survival motor neuron.

[1]Mean weights in grams from five SMNΔ7 mice and six controls studied with daily CMAP and MUNE measurements between ages 3 and 13 days.

[2]This correction factor is based on assumption of similar polyneuronal innervation pruning.[39,43]

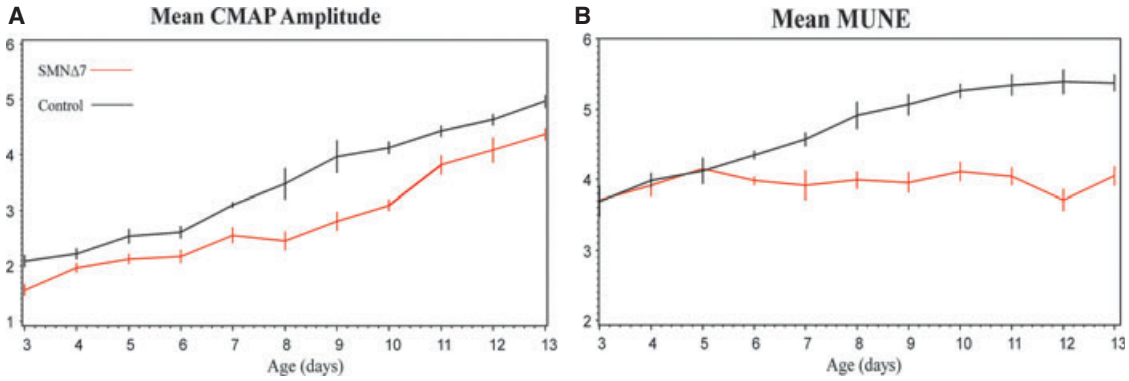

Figure 2. Transformed longitudinal CMAP (square root) and MUNE (logarithm) measurements in untreated SMNΔ7 and control mice. (A) Sciatic CMAP amplitude shows a divergent drop in SMNΔ7 mice and amplitude is significantly reduced at 6–13 days ($P < 0.01$). There is partial recovery of CMAP amplitude at days 11–13. (B) Sciatic MUNE is similar in SMNΔ7 mice and controls at early postnatal time points. There is progressive motor unit loss beginning at PND 6 that reaches statistical significance reduced on days 7–13 ($P < 0.01$). CMAP, compound muscle action potential; MUNE, motor unit number estimation; SMN, survival motor neuron; PND, postnatal day.

and MUNE in $ChAT^{Cre}$ mice ($n = 10$; 20.4 ± 1.8 mV and 138 ± 21 mV) compared with controls ($n = 13$; 44.0 ± 2.9 mV and 283 ± 15 mV) ($P < 0.001$). EMG shows fibrillation potentials in hind limb muscles (4 of 5 $ChAT^{Cre}$ and 0 of 5 controls) ($P = 0.02$).

Electrophysiological measurements following therapy to restore SMN

CMAP and MUNE responses were obtained in SMNΔ7 mice ($n = 7$) on day 12 following ASO therapy and com-

Table 3. 2 × 2 contingency table of presence or absence of fibrillations.

Genotype	Fibrillations	No fibrillations
Control	0	5
SMNΔ7	6	1

EMG revealed the presence of fibrillations due to denervation in SMA mice but not control mice. A Fisher exact test for the expected distribution indicates a significant difference between the groups, $P = 0.015$ (statpages.org/ctab 2x2.html). SMN, survival motor neuron; EMG, electromyography; SMA, spinal muscular atrophy.

pared with untreated SMNΔ7 ($n = 8$) and treated control mice ($n = 7$) (Fig. 4). At 12 days, MUNE responses are significantly improved in treated SMNΔ7 mice (189 ± 31) compared with untreated SMNΔ7 mice (47 ± 6) ($P = 0.0045$). There was no significant improvement in CMAP responses in treated SMNΔ7 mice (16.6 ± 1.0 mV) 12 days following treatment compared to untreated SMNΔ7 mice (16.8 ± 1.6 mV) ($P = 0.6742$). Additional CMAP and MUNE responses were also obtained at PND 30 for comparison (Fig. 4). At 30 days post injection, MUNE and CMAP in treated SMNΔ7 (CMAP: 33.5 ± 3.4; MUNE: 217 ± 44) and control mice (CMAP: 36.2 ± 1.8; MUNE: 325 ± 36) are similar (CMAP: $P = 0.4822$; MUNE: $P = 0.0733$). At 30 days post injection, untreated SMNΔ7 mice expired and were not available for comparison. Needle EMG at 90 days post injection demonstrated no fibrillation potentials in treated SMNΔ7 mice ($n = 5$) or untreated controls ($n = 3$).

Similar findings of CMAP and MUNE correction were seen in measurements at PND 165 performed on SMNΔ7 mice that received SMN full length cDNA via AAV9-mediated gene transfer[39] (two animals, studied bilaterally, $n = 4$, unblinded). Consistent with findings after ASO treatment, CMAP (treated SMNΔ7: mean 51.0±2.2 mV; controls mean 48.1 ± 2.4) and MUNE (treated SMNΔ7: mean 225 ± 22; controls: mean 236 ± 28) measurements were not significantly different compared to controls (CMAP: $P = 0.625$; MUNE: $P = 0.875$). Needle EMG demonstrated no fibrillation potentials.

Discussion

We have modified CMAP and MUNE techniques for the investigation of motor unit function in vivo in SMA mouse models at time points as early as PND 3. These techniques can be used to understand events of early motor unit development and dysfunction at the onset of the SMA phenotype. CMAP and MUNE in the early postnatal period are similar between SMNΔ7 and control mice. CMAP and MUNE responses are significantly reduced in SMNΔ7 mice in correlation with the onset of overt motor phenotype.[15,16] Prior morphological assessment of the SMNΔ7 mouse has shown mild to severe denervation and moderate motor neuron loss that varies by spinal cord segment and muscles assessed. For the gastrocnemius (one of the muscles assayed with CMAP and MUNE), Le et al. showed increased non innervated and partial innervated NMJ's in the gastrocnemius.[15] Kariya et al. did not show denervation in the gastrocnemius but showed in this same muscle that 90% of nerve terminals are thick/swollen, a condition that could lead to decreased function.[43] Furthermore Bäumer et al. showed motor neuron loss in the lumbar cord that was detectable at 7 days in SMNΔ7 mice (correlating with our findings of significantly reduced MUNE) and 35% loss at later stages.[44] While Kong et al. showed mild complete denervation, partial or abnormal terminals were not scored in most muscles.[26] Ling et al. showed variable denervation in a series of muscles, but most of the muscles assayed

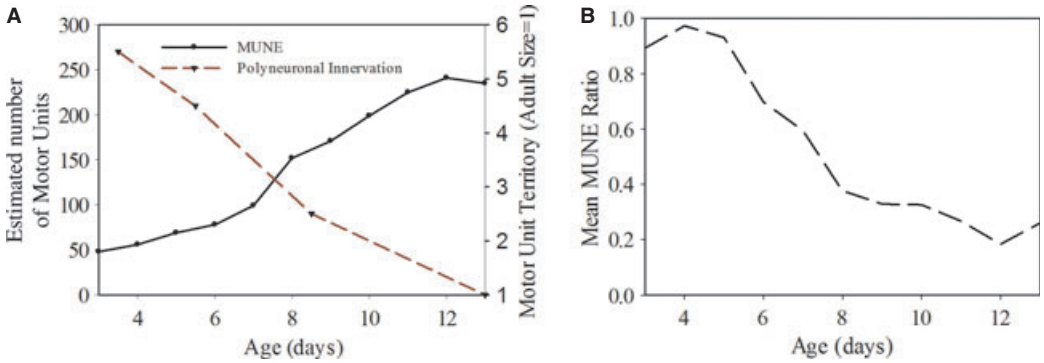

Figure 3. Polyneuronal innervation effect on MUNE response. (A) Correlation of the rate of polyneuronal innervation pruning with increasing MUNE responses in control mice. (B) Plot of MUNE ratio (SMNΔ7 vs. control), to correct for polyneuronal innervation, to demonstrate onset and progression of motor unit degeneration in SMNΔ7 mice. CMAP, compound muscle action potential; MUNE, motor unit number estimation; SMN, survival motor neuron.

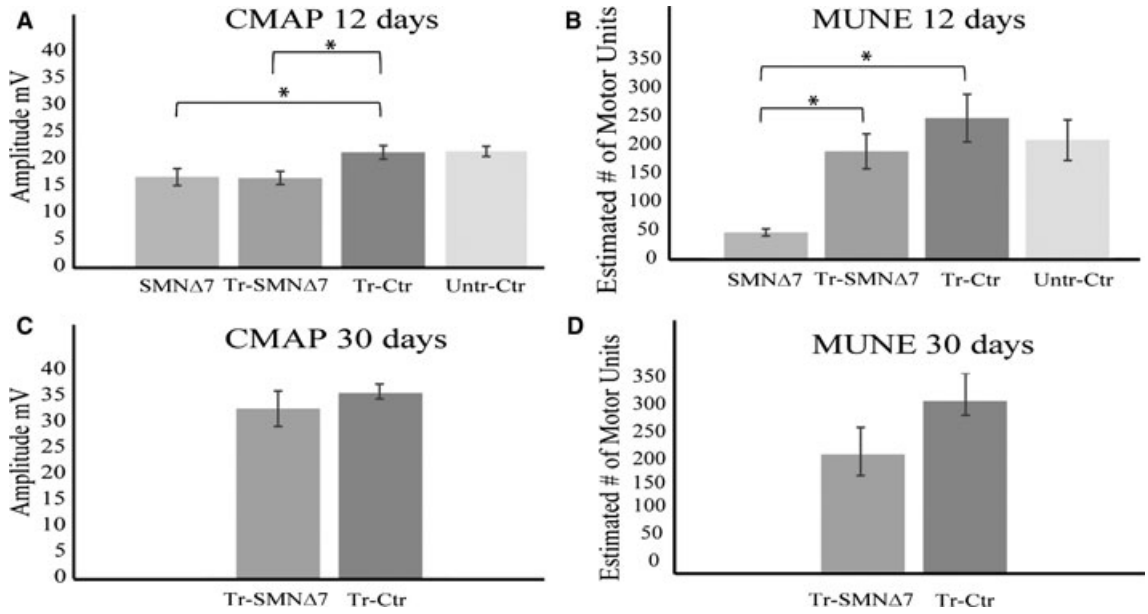

Figure 4. CMAP and MUNE at 12 and 30 days following SMN restoration with ASO. (A) At 12 days, CMAP amplitudes are significantly reduced in untreated and treated SMNΔ7 mice compared with controls. There is no significant difference between treated and untreated SMNΔ7 mice. (B) At 12 days, MUNE is significantly higher in treated SMNΔ7 mice compared with untreated SMNΔ7 mice. There is no significant difference between treated SMNΔ7 mice and controls. $*P < 0.01$. (C) At 30 days, CMAP amplitudes are similar between treated SMNΔ7 mice and controls ($P = 0.4822$). (D) At 30 days, MUNE is slightly reduced in treated SMNΔ7 mice, but this does not reach statistical significance ($P = 0.0733$). CMAP, compound muscle action potential; MUNE, motor unit number estimation; SMN, survival motor neuron; ASO, antisense oligonucleotide; SMNΔ7, untreated SMNΔ7; Tr-SMNΔ7, antisense oligonucleotide treated SMNΔ7; Tr-Ctr, antisense oligonucleotide treated controls; Untr-Ctr, untreated controls.

with our techniques of sciatic CMAP and MUNE were not assessed in this study.[45] Specifically, two of the three muscles assayed by Ling et al. that are innervated by the sciatic nerve, flexor digitorum brevis 2 and 3, showed significant denervation at P7 (correlating with MUNE) with only 31% of muscle fibers remaining fully innervated.[45] Therefore, the findings of significant reduction in estimated functional motor units (as measured by MUNE) in SMNΔ7 mice are particularly interesting and important as these findings may suggest that function does not parallel morphology in this rapidly progressive model.

The incongruent electrophysiological findings of significantly reduced neuromuscular function in SMNΔ7 mice compared with variable histological findings of minimal to severe denervation could represent artifact of either electrophysiological or morphological techniques or a combination. CMAP and MUNE are well-established clinical techniques that provide an assessment of neuromuscular function, in vivo. The phenomenon of polyneuronal innervation has been suggested as a potential confounding source of artifact in morphological evaluation of denervation in SMA mouse models.[40] In contrast to our findings, Lee et al. reported reduced total muscle force from the soleus muscle but no differences in the number functional motor units in control and SMNΔ7 soleus muscles at end stage.[39] As the techniques of sciatic MUNE and CMAP in mice measure numerous sciatic-innervated muscles, it remains unclear how our findings are related to measures in one muscle at one time point. In the study by Lee et al., increments in muscle twitch tension were used to determine the number of motor units in control and SMNΔ7 soleus muscles.[39] This technique identified a relatively sparse number of motor units (~14) in both SMNΔ7 and control soleus muscles. This raises the question of whether there was inadequate resolution of this twitch tension assay for identifying motor units, particularly those that represent a small percentage of the total muscle tension. Furthermore, our MUNE results demonstrate an expansion of individual motor unit territory in the SMNΔ7 mice that leads to each motor unit representing a larger percentage of the total output. It is possible that these factors could lead to increased bias of incremental twitch tension assay toward lower motor unit estimates in controls with nonenlarged motor units.

The *ChAT*^{Cre} driver has previously been shown to give good expression in motor neurons.[29] We have used this driver to remove mouse *Smn* from motor neurons and make them solely dependent on SMN from two copies of *SMN2*. In this instance other tissues, including muscle,

have carrier levels of SMN. In the $ChAT^{Cre}$ mice, with mouse *Smn* removed from motor neurons and reliant on SMN2, electrophysiological measurements showed reduced CMAP and MUNE as well as fibrillations at 21 days. The findings at 21 days in $ChAT^{Cre}$ mice, similar to those in SMNΔ7 mice, are consistent with loss of motor unit function. Although delayed polyneuronal innervation pruning could also explain the failure of MUNE numbers to increase in SMNΔ7 mice, the findings in $ChAT^{Cre}$ mice at 21 days argue against this possibility.

A major advantage of CMAP as a biomarker is the simplicity of the technique. CMAP size is affected by pathological processes involving the motor neuron, axon, synapse, or the muscle. CMAP is a measure of the output from the motor neurons supplying a muscle, and an indirect measure of motor neuron function. This can be considered an advantage of the technique; however, it is also a limitation. The nonspecificity of the CMAP measurement does not allow localization of pathological processes (or mechanism of rescue) to the axon, NMJ, or muscle. Furthermore, abnormalities in the CMAP response may be absent in the presence of partial denervation. During slowly progressive denervation in human disease or animal models, the remaining motor units may increase their territories to reinnervate muscle fibers that have lost synaptic input, and in certain instances reinnervation may be sufficient to normalize the CMAP response. Furthermore, it is expected that this compensatory mechanism is greater in mouse models than in humans due to shorter axon length, and our studies in the SMNΔ7 mouse are consistent with this expectation. Therefore, in animal models with significant reinnervation capacity, CMAP may be a less sensitive measure. MUNE accounts for reinnervation and changes in muscle tissue to give a more direct assessment of the number of functional motor units. Although similarly non-invasive, MUNE is more time-consuming with additional technical considerations, and may be less optimal in multicenter clinical applications in infants and young children.

SMA has pathological features suggestive of both a developmental and neurodegenerative disorder.[46] The findings of preserved MUNE responses in rescued SMNΔ7 mice compared with non-treated SMNΔ7 mice are consistent with prevention of motor unit degeneration. Interestingly the CMAP responses remain reduced in the treated SMA animals at 12 days following ASO injection suggesting reduction in the output of the rescued motor units. At 30 days post injection, the output of the motor units in rescued animals shows normalization of the CMAP. Thus, there is gradual return of normal motor unit output with time after SMN restoration. Early SMN restoration appears to halt motor unit loss, but restoration of the function of the motor unit is delayed as demonstrated by gradual return of CMAP amplitude in rescued SMNΔ7 mice. This suggests that in early clinical trials the disease progression (i.e., motor unit loss) may be halted with SMN therapies but development of improved motor unit output (and thus improvement of functional outcomes) may be more gradual or delayed. This finding parallels the ex vivo synaptic recordings reported by Foust et al. following rescue with AAV9-SMN showing partial electrophysiological correction at day 10 post injection and delayed normalization.[47] Therefore longitudinal measurements will be needed, and a longer postintervention follow-up interval may be required to see the full effects of SMN restoration.

Several promising preclinical treatments targeting SMN restoration have demonstrated dramatic rescue of the SMA phenotype and extension of survival in mouse models. Importantly, SMN-restoring therapies demonstrate diminishing efficacy with delayed delivery consistent with the concept of a therapeutic window of opportunity for SMN-targeting therapies.[19] Whether there is a similar therapeutic window in human SMA is unknown. Effective biomarkers are needed to accurately identify appropriate timing to obtain maximal SMN-restoring effects with these therapeutics. These measures must assess the function of the neuromuscular system and provide predictive information about the potential for SMN-restoring therapies to provide a rescue effect. Furthermore, when CMAP and MUNE are already severely reduced the effect of SMN restoration is expected to be diminished. Therefore, these measures can potentially be used to stratify treatment strategies and predict disease response. In the future, these biomarkers can be applied in different mouse models to understand the pattern of motor unit loss and response to treatment.

The techniques described here measure motor unit function in a preclinical model of SMA using methods that parallel those predicted to be used in future clinical trials. We have shown that these techniques can identify loss of motor unit function in the SMNΔ7 mouse model mirroring those seen in patients with SMA. Most importantly, we demonstrate that these markers show improvement with rescue of the SMA phenotype, and this study provides proof of concept of CMAP and MUNE as biomarkers of outcome. The work here provides robust support for the twofold application of CMAP and MUNE as endpoint measures in preclinical studies to facilitate effective translation to early clinical trials and as effective biomarkers for use in early clinical trials for SMA.

Acknowledgment

This study was supported by funding from NIH 5K12HD001097-17 to W. D. A., the Swiss National

Science Foundation to K. M., NIH/NINDS U01NS080836 to B. K. K., Families of SMA to B. K. K., Sophia's cure to B. K. K., NIH/NINDS K08NS067282 and U01NS079163 to S. J. K., and NIH HD006508 to A. H. M. B.

Authorship

WDA, SJK, JTK, and AHB designed the study. WDA designed the modified electrophysiological techniques and conducted all electrophysiological measurements. VLM, CCI, SD performed mouse genotyping and blinding for electrophysiology. PNP performed ICV injections. XL performed statistical modeling and analysis. KM, LS, and BKK designed and performed ICV gene therapy injections. WDA and AHB were involved with drafting of the manuscript. All authors assisted in revision and provided final approval of the manuscript.

Conflict of Interest

Dr. Kaspar has patents, AAV9 and blood brain barrier/CSF barrier, licensed to AveXis Inc., and a patent, AAV9 SMN, licensed to AveXis Inc.

References

1. Roberts DF, Chavez J, Court SD. The genetic component in child mortality. Arch Dis Child 1970;45:33–38.
2. Lefebvre S, Burglen L, Reboullet S, et al. Identification and characterization of a spinal muscular atrophy-determining gene. Cell 1995;80:155–165.
3. Monani UR, Lorson CL, Parsons DW, et al. A single nucleotide difference that alters splicing patterns distinguishes the SMA gene SMN1 from the copy gene SMN2. Hum Mol Genet 1999;8:1177–1183.
4. Lorson CL, Hahnen E, Androphy EJ, Wirth B. A single nucleotide in the SMN gene regulates splicing and is responsible for spinal muscular atrophy. Proc Natl Acad Sci USA 1999;96:6307–6311.
5. Cartegni L, Krainer AR. Disruption of an SF2/ASF-dependent exonic splicing enhancer in SMN2 causes spinal muscular atrophy in the absence of SMN1. Nat Genet 2002;30:377–384.
6. Lorson CL, Strasswimmer J, Yao JM, et al. SMN oligomerization defect correlates with spinal muscular atrophy severity. Nat Genet 1998;19:63–66.
7. Burnett BG, Munoz E, Tandon A, et al. Regulation of SMN protein stability. Mol Cell Biol 2009;29:1107–1115.
8. McAndrew PE, Parsons DW, Simard LR, et al. Identification of proximal spinal muscular atrophy carriers and patients by analysis of SMNT and SMNC gene copy number. Am J Hum Genet 1997;60:1411–1422.
9. Burghes AH. When is a deletion not a deletion? When it is converted. Am J Hum Genet 1997;61:9–15.
10. Burghes AH, Beattie CE. Spinal muscular atrophy: why do low levels of survival motor neuron protein make motor neurons sick? [Review] [171 refs]. Nat Rev Neurosci 2009;10:597–609.
11. Pellizzoni L. Chaperoning ribonucleoprotein biogenesis in health and disease. EMBO Rep 2007;8:340–345.
12. Rossoll W, Jablonka S, Andreassi C, et al. SMN, the spinal muscular atrophy-determining gene product, modulates axon growth and localization of beta-actin mRNA in growth cones of motoneurons. J Cell Biol 2003;163:801–812.
13. McWhorter ML, Monani UR, Burghes AH, Beattie CE. Knockdown of the survival motor neuron (SMN) protein in zebrafish causes defects in motor axon outgrowth and pathfinding. J Cell Biol 2003;162:919–932.
14. Rossoll W, Bassell GJ. Spinal muscular atrophy and a model for survival of motor neuron protein function in axonal ribonucleoprotein complexes. Results Probl Cell Differ 2009;48:289–326.
15. Le TT, Pham LT, Butchbach MER, et al. SMNΔ7, the major product of the centromeric survival motor neuron (SMN2) gene, extends survival in mice with spinal muscular atrophy and associates with full-length SMN. Hum Mol Genet 2005;14:845–857.
16. Butchbach ME, Edwards JD, Burghes AH. Abnormal motor phenotype in the SMNDelta7 mouse model of spinal muscular atrophy. Neurobiol Dis 2007;27:207–219.
17. Le TT, McGovern VL, Alwine IE, et al. Temporal requirement for high SMN expression in SMA mice. Hum Mol Genet 2011;20:3578–3591.
18. Lutz CM, Kariya S, Patruni S, et al. Postsymptomatic restoration of SMN rescues the disease phenotype in a mouse model of severe spinal muscular atrophy. J Clin Invest 2011;121:3029–3041.
19. Arnold WD, Burghes AH. Spinal muscular atrophy: the development and implementation of potential treatments. Ann Neurol 2013;74:348–362.
20. Buchthal F, Olsen PZ. Electromyography and muscle biopsy in infantile spinal muscular atrophy. Brain 1970;93:15–30.
21. Hausmanowa-Petrusewicz I, Karwańska A. Electromyographic findings in different forms of infantile and juvenile proximal spinal muscular atrophy. Muscle Nerve 1986;9:37–46.
22. Swoboda KJ, Prior TW, Scott CB, et al. Natural history of denervation in SMA: relation to age, SMN2 copy number, and function. Ann Neurol 2005;57:704–712.
23. Lewelt A, Krosschell KJ, Scott C, et al. Compound muscle action potential and motor function in children with spinal muscular atrophy. Muscle Nerve 2010;42:703–708.
24. Kaufmann P, McDermott MP, Darras BT, et al. Prospective cohort study of spinal muscular atrophy types 2 and 3. Neurology 2012;79:1889–1897.

25. Finkel RS. Electrophysiological and motor function scale association in a pre-symptomatic infant with spinal muscular atrophy type I. Neuromuscul Disord 2013;23:112–115.
26. Kong L, Wang X, Choe DW, et al. Impaired synaptic vesicle release and immaturity of neuromuscular junctions in spinal muscular atrophy mice. J Neurosci 2009;29:842–851.
27. Ling KKY, Lin M-Y, Zingg B, et al. Synaptic defects in the spinal and neuromuscular circuitry in a mouse model of spinal muscular atrophy. PLoS One 2010;5:e15457.
28. Cifuentes-Diaz C, Frugier T, Tiziano FD, et al. Deletion of murine SMN exon 7 directed to skeletal muscle leads to severe muscular dystrophy. J Cell Biol 2001;152:1107–1114.
29. Paez-Colasante X, Seaberg B, Martinez TL, et al. Improvement of neuromuscular synaptic phenotypes without enhanced survival and motor function in severe spinal muscular atrophy mice selectively rescued in motor neurons. PLoS One 2013;8:e75866.
30. Schrank B, Götz R, Gunnersen JM, et al. Inactivation of the survival motor neuron gene, a candidate gene for human spinal muscular atrophy, leads to massive cell death in early mouse embryos. Proc Natl Acad Sci USA 1997;94:9920–9925.
31. Tapia JC, Wylie JD, Kasthuri N, et al. Pervasive synaptic branch removal in the mammalian neuromuscular system at birth. Neuron 2012;74:816–829.
32. Shefner JM, Cudkowicz ME, Brown RH. Comparison of incremental with multipoint MUNE methods in transgenic ALS mice. Muscle Nerve 2002;25:39–42.
33. Shefner JM, Cudkowicz M, Brown RH. Motor unit number estimation predicts disease onset and survival in a transgenic mouse model of amyotrophic lateral sclerosis. Muscle Nerve 2006;34:603–607.
34. Xia RH, Yosef N, Ubogu EE. Dorsal caudal tail and sciatic motor nerve conduction studies in adult mice: technical aspects and normative data. Muscle Nerve 2010;41:850–856.
35. Srivastava AK, Renusch SR, Naiman NE, et al. Mutant HSPB1 overexpression in neurons is sufficient to cause age-related motor neuronopathy in mice. Neurobiol Dis 2012;47:163–173.
36. Nandedkar SD, Barkhaus PE. Contribution of reference electrode to the compound muscle action potential. Muscle Nerve 2007;36:87–92.
37. Porensky PN, Mitrpant C, McGovern VL, et al. A single administration of morpholino antisense oligomer rescues spinal muscular atrophy in the mouse. Hum Mol Genet 2012;21:1625–1638.
38. Parano E, Uncini A, De Vivo DC, Lovelace RE. Electrophysiologic correlates of peripheral nervous system maturation in infancy and childhood. J Child Neurol 1993;8:336–338.
39. Lee YI, Mikesh M, Smith I, et al. Muscles in a mouse model of spinal muscular atrophy show profound defects in neuromuscular development even in the absence of failure in neuromuscular transmission or loss of motor neurons. Dev Biol 2011;356:432–444.
40. Murray LM, Comley LH, Thomson D, et al. Selective vulnerability of motor neurons and dissociation of pre- and post-synaptic pathology at the neuromuscular junction in mouse models of spinal muscular atrophy. Hum Mol Genet 2008;17:949–962.
41. Ruiz R, Casanas JJ, Torres-Benito L, et al. Altered intracellular Ca^{2+} homeostasis in nerve terminals of severe spinal muscular atrophy mice. J Neurosci 2010;30:849–857.
42. Gramsbergen A, IJkema-Paassen J, Nikkels PG, Hadders-Algra M. Regression of polyneural innervation in the human psoas muscle. Early Hum Dev 1997;49:49–61.
43. Kariya S, Park GH, Maeno-Hikichi Y, et al. Reduced SMN protein impairs maturation of the neuromuscular junctions in mouse models of spinal muscular atrophy. Hum Mol Genet 2008;17:2552–2569.
44. Bäumer D, Lee S, Nicholson G, et al. Alternative splicing events are a late feature of pathology in a mouse model of spinal muscular atrophy. PLoS Genet 2009;5:e1000773.
45. Ling KK, Gibbs RM, Feng Z, Ko CP. Severe neuromuscular denervation of clinically relevant muscles in a mouse model of spinal muscular atrophy. Hum Mol Genet 2012;21:185–195.
46. Crawford TO, Pardo CA. The neurobiology of childhood spinal muscular atrophy. Neurobiol Dis 1996;3:97–110.
47. Foust KD, Wang X, McGovern VL, et al. Rescue of the spinal muscular atrophy phenotype in a mouse model by early postnatal delivery of SMN. Nat Biotechnol 2010;28:271–274.

Supporting Information

Additional Supporting Information may be found in the online version of this article:

Figure S1. Illustration of electrophysiological assessment of the motor unit pool, in vivo. MUNE, motor unit number estimation; CMAP, compound muscle action potential; EMG, electromyography; RNS, repetitive nerve stimulation .

